CURRENT BASED DISTANCE PROTECTION IN CLOSED-RING GRIDS WITH DISTRIBUTED GENERATION

Martin BILLER
FAU University Erlangen-Nuremberg – Germany
martin.biller@fau.de

Johann JAEGER
FAU University Erlangen-Nuremberg – Germany
johann.jaeger@fau.de

ABSTRACT

Conventional methods of distance protection relays measure an impedance. Based on voltages and currents, the relay determines the distance between relay and fault location and enables selective fault clearing. Closed-ring structures increase the grid capacity for connecting distributed energy resources as inter infeeds. However, closed-ring structures and inter infeeds can cause malfunctions of conventional distance protection and disturb the proper operation of non-directional short-circuit current indicators particularly. This paper proposes a current based distance protection method that complies with closed loop structures and inter infeeds properly in case of unbalanced faults. The proposed approach is based on current comparison and negative-sequence system quantities. Thus, it remains unaffected from inter infeeds and fault resistances. The approach serves as a supplement to conventional distance protection methods which are applied for symmetrical faults and if the closed-ring structure is dissolved. Finally, the paper presents a protection grading strategy that significantly reduces the average fault clearing time.

INTRODUCTION

Grids are more and more penetrated with high shares of distributed energy resources (DER). Thus, open-loop structures may be preferably operated as closed loops in order to balance voltage and load profiles. This change of topology from open-loop to closed-loop structures may delay or even avoid necessary grid expansions.
The conventional distance protection principle measures voltages and phase currents at the relay location and calculates impedances for phase-to-phase and phase-to-earth loops. These impedances represent the distance between the relay and the fault location in the best case [1]. However, the impedance measurement can be strongly falsified if inter infeed at the faulted line, infeed from the remote end of a loop or high fault resistances occur.
State of the art knows methods that can mitigate some of those adverse effects. Distance protection relays may use only the reactive part of the measured impedance to remedy the impact of high fault resistances [1]. Fault resistances in combination with infeed from remote end are also manageable, e.g. with the approaches presented in [2], [3] and [4]. However, these approaches are mainly based on the method presented in [5]. This means these methods attempt to compensate the impact of the voltage drop across the fault. Another method used for improved fault locating in parallel transmission lines is presented in [6].

Nevertheless, if all these adverse effects occur simultaneously, handling fault events can be very difficult. Particularly the inter infeed problem remains unsolved for those approaches. Distance protection relays are not equipped with a communication channel to the DER. Consequently, the distance protection relay does not know to what extent weather- and time-of-day-dependent DER, such as windmills or PV plants, feed in at the moment the fault occurs. This means, the additional voltage drop caused by the DER is unknown. Thus, the inter infeed effect is unavoidable as well as unpredictable for the relay and affects “state of the art” relays adversely.
The proposed current based distance protection method overcomes these problems for unbalanced faults. It applies an algorithm mainly based on the comparison of negative-sequence currents measured at the relay locations at the loop ends. Measured voltages are not needed anymore. Thus, the additional voltage drop does not affect the method.
Moreover, a new strategy for protection grading in closed-loop structures is introduced in accordance with on the current based distance protection method. It helps to reduce the fault clearing times in closed loop structures.

PROTECTION SYSTEMS CHALLENGES IN CLOSED-RING GRIDS WITH DISTRIBUTED GENERATION

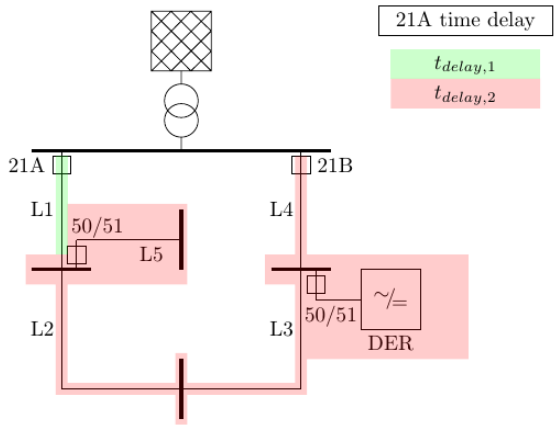

Fig. 1: Closed-Ring Distribution Grid Structure with Conventional Protection System

The most significant challenges for the protection system in closed-ring structures in distribution grids with distributed generation are the adverse impacts of the inter infeed effect, the insufficient performance of conventional protection grading strategies in terms of fault clearing times and difficulties in locating the fault.
Fig. 1 illustrates these problems. It shows an exemplary

distribution grid in a closed-ring structure that consists of a ring of four lines L1, L2, L3 and L4. A lateral feeder L5 and a DER are connected to the ring. The ring is protected by two distance protection relays installed at the busbar. Both the lateral feeder L5 and the DER are separately protected by time overcurrent protection. The busbar relays provide backup protection for those relays.

Inter Infeed Effect

One main problem of the inter infeed effect is causing measurement errors in distance protection relays. The severity of the measurement error depends on magnitude and angle of the inter infeed and on the relative location of protection relay, inter infeed and fault location to each other [1], [7]. On the one hand the relay does not know the impedances between inter infeed and fault location. On the other hand, particularly for windmills and PV plants the magnitude and angle of the DER inter infeed is not known to the relay. This means, these two influence quantities cannot be factored in the impedance calculation properly. Additionally, due to fault ride through (FRT) regulations, DER infeed is highly variable even during the fault clearing period. Therefore, the DER adversely affects the conventional distance protection relays 21A and 21B in Fig. 1.

Protection Grading Strategy

In Fig. 1, the coloured areas show after what time delay relay 21A trips. Green is for the shortest time delay $t_{delay,1}$, red for the longer time delay $t_{delay,2}$. In order to avoid overfunction for faults on the lateral feeder L5 and with respect to inaccuracies in CT and VT measurements as well as in asset data, the zone for $t_{delay,1}$ must be restricted to a little before the node where L5 is connected. This means, all faults on the ring behind that node (on lines L2, L3, L4) are cleared after $t_{delay,2}$. Relay 21B has similar restraints due to the DER connected between L3 and L4. Considering all faults on the ring are only cleared if both busbar relays 21A and 21B trip, this means all faults on the ring are cleared in $t_{delay,2}$ only; even if one of the relays trips in $t_{delay,1}$. This prolonged average fault clearing time ring may interfere with the FRT through capabilities of DER and thus can lead to an unwanted additional loss of distributed generation.

Fault Locating

Many distribution grids, especially in rural areas, rely on non-directional short-circuit indicators to identify the faulty section after a fault has been cleared. This is not applicable in closed-ring structures because all faults on the ring are fed by two sides. All short-circuit indicators may be affected by the short-circuit current and thus lose the ability to locate the faulty section. This and hardens the job for service and maintenance crews and means longer periods of loss of supply for the costumers.

BASIC PRINCIPLE

The current based distance protection approach proposed in this paper is based on current comparison and can be used for clearing and locating unbalanced faults in closed-ring structures. As it is an essential requirement for the proposed approach, the relays are assumed to be interconnected and can interchange current measurement signals like shown in Fig. 5.

The negative-sequence currents sensed by the relays installed at the busbar are summed up and the relative share of each relay to that sum is calculated. This share is called the relative fault current contribution (FCC) and can be calculated with (1) and (2) for each relay respectively.

$$FCC_A = Re\left\{\frac{\underline{I}_{A(2)}}{\underline{I}_{A(2)} + \underline{I}_{B(2)}}\right\} \quad (1)$$

$$FCC_B = Re\left\{\frac{\underline{I}_{B(2)}}{\underline{I}_{A(2)} + \underline{I}_{B(2)}}\right\} \quad (2)$$

Fig. 2 shows the negative-sequence equivalent circuit for the network in Fig. 1. For every fault on the ring (lines L1, L2, L3 and L4), on the lateral feeder L5 or within the DER, the fault current in the negative-sequence system $\underline{I}_F$ distributes in a certain ratio through the relays A and B at the busbar and thus leads to a specific FCC for each relay for every fault location. Assuming a fault at fault location F, the fault current $\underline{I}_F$ flows through the negative-sequence network via three paths: One is via $\underline{Z}_2$, $\underline{Z}_1$ and $\underline{Z}_{Src(2)}$, the current is measured by relay A. Another one is via $\underline{Z}_3$, $\underline{Z}_4$ and $\underline{Z}_{Src(2)}$. That current is measured by relay B. The last path is via $\underline{Z}_3$ and $\underline{Z}_{DER(2)}$ whose current is not sensed by any of the relays installed at the busbar since $\underline{Z}_{DER(2)}$ bypasses relays A and B.

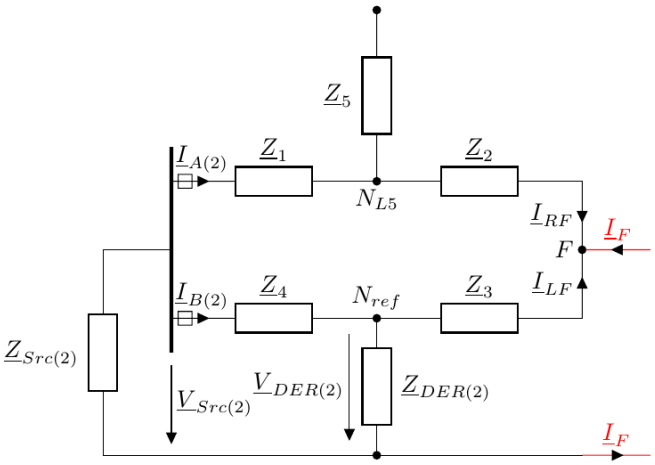

Fig. 2: Negative-Sequence Equivalent Circuit for Exemplary Network from Fig. 1

Rough Fault Localization: Detection of the Faulty Ring Section

For every node that offers such a significantly little lateral impedance in the negative-sequence system to bypass the

source impedance (i.e. the busbar relays), a referential pre-calculation for the FCC must be performed. For Fig. 2 this is the case for node N_{ref} where the DER is connected. This is done by applying an unbalanced fault at N_{ref} (e.g. using software simulation) and hence recording the $FCC_{A,Nref}$ and $FCC_{B,Nref}$ for both relays using (1) and (2). Since the negative-sequence network contains no current or voltage sources and all impedances can be considered constant [8], both FCC_{Nref} are dependent from arrangement of the negative-sequence impedances only. This arrangement remains unaffected from all actions not taking place in the negative-sequence system network. Consequently, the FCC_{Nref} lead to the exact same result for all types of unbalanced faults at node N_{ref}. The magnitude and phase angle of the fault current do not affect the FCC_{Nref}.
The proposed method sections the ring by every node with a significantly little lateral impedance. In Fig. 2 these nodes are the busbar and N_{ref}. Consequently, the ring consists of the two sections from the relays A and B to node N_{ref}. The ring sections and the corresponding section line impedances are shown in Table 1. Note that the source impedance and the impedances of the lateral feeder L5 and the DER are not considered to be part of the ring sections. Only the line impedances of the ring are considered.

Table 1: Ring Sections and Corresponding Line Impedances

Name of Ring Section	Section Line Impedance
A_N_{ref}	$\underline{Z}_{A\_N_{ref}} = \underline{Z}_1 + \underline{Z}_2 + \underline{Z}_3$
B_N_{ref}	$\underline{Z}_{B\_N_{ref}} = \underline{Z}_4$

In case of a fault, the FCC of both relays are compared to the corresponding referential $FCC_{A,Nref}$ and $FCC_{B,Nref}$ to detect the faulty section. The logic performing that task is shown in Table 2. The higher the value of the FCC sensed by a relay, the closer the fault location is to that relay. By this means, a rough fault localization is performed. This allows the DSO to identify the faulty ring section from the grid in a first step to isolate the fault.

Table 2: Faulty Section Decision Logic

FCC_A	FCC_B	Faulty Section
$> FCC_{A,Nref}$	$< FCC_{B,Nref}$	A_N_{ref}
$< FCC_{B,Nref}$	$> FCC_{B,Nref}$	B_N_{ref}

In the case from Fig. 2 the fault occurs at fault location F. Thus, FCC_A is bigger than $FCC_{A,Nref}$ and FCC_B is smaller than $FCC_{B,Nref}$. The logic concludes the faulty ring section to be section A_N_{ref}. The fault location thus is assumed to be somewhere between relay A and node N_{ref}.

Precise Fault Localization: Determination of the Impedance between Relays and Fault Location

After the faulty ring section is determined, the left-hand and right-hand sided currents from the fault location $\underline{I}_{LF}$ and $\underline{I}_{RF}$ as shown in Fig. 2 are calculated for a more precise identification of the actual fault location. Prerequisite is knowledge of the values of all section line impedances of the ring sections, significantly small lateral impedances and the negative-sequence currents at the relays $\underline{I}_{A(2)}$ and $\underline{I}_{B(2)}$. With this data basis, $\underline{I}_{LF}$ and $\underline{I}_{RF}$ are calculated.
Referring to Fig. 2, $\underline{I}_{LF}$ and $\underline{I}_{RF}$ are calculated with equations (3), (4), (5) and (6).

$$\underline{V}_{Src(2)} = -\left(\underline{I}_{A(2)} + \underline{I}_{B(2)}\right) \cdot \underline{Z}_{Src(2)} \quad (3)$$

$$\underline{V}_{DER(2)} = \underline{V}_{Src(2)} - \underline{I}_{B(2)} \cdot \underline{Z}_{B\_N_{ref}} \quad (4)$$

$$\underline{I}_{LF(2)} = \underline{I}_{B(2)} - \frac{\underline{V}_{DER(2)}}{\underline{Z}_{DER(2)}} \quad (5)$$

$$\underline{I}_{RF(2)} = \underline{I}_{A(2)} \quad (6)$$

Since the fault occurs in section A_N_{ref}, the corresponding section impedance $\underline{Z}_{A\_N_{ref}}$ is split into two impedances by the fault. This is shown in Fig. 3. The left-hand and right-hand side impedances to the fault location are named $\underline{Z}_{LF}$ and $\underline{Z}_{RF}$. They describe the impedances from the fault to the next significantly small lateral impedances. In our case these are $\underline{Z}_{DER(2)}$ on the left and $\underline{Z}_{Src(2)}$ on the right.

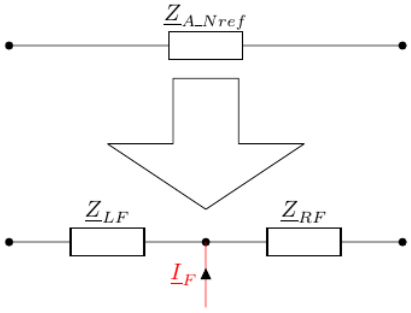

Fig. 3: Split of Ring Section Impedance in Case of Fault

According to the equivalent circuit in Fig. 2, $\underline{Z}_{LF}$ and $\underline{Z}_{RF}$ can be calculated with (7), (8), (9) and (10). Note that, if (9) is known, (10) is redundant and vice versa.

$$\underline{V}_{Src(2)} - \underline{Z}_{RF} \cdot \underline{I}_{RF(2)} = \underline{V}_{DER(2)} - \underline{Z}_{LF} \cdot \underline{I}_{LF(2)} \quad (7)$$

$$\underline{Z}_{LF} + \underline{Z}_{RF} = \underline{Z}_{A\_N_{ref}} \quad (8)$$

$$\underline{Z}_{RF} = \frac{\underline{V}_{Src(2)} - \underline{V}_{DER(2)} + \underline{I}_{LF(2)} \cdot \underline{Z}_{A\_N_{ref}}}{\underline{I}_{LF(2)} + \underline{I}_{RF(2)}} \quad (9)$$

$$\underline{Z}_{LF} = \frac{\underline{V}_{DER(2)} - \underline{V}_{Src(2)} + \underline{I}_{RF(2)} \cdot \underline{Z}_{A\_N_{ref}}}{\underline{I}_{LF(2)} + \underline{I}_{RF(2)}} \quad (10)$$

By this means, the line impedances from the relays to the fault location can be calculated with (11) and (12).

$$\underline{Z}_{AF} = \underline{Z}_{RF} = \underline{Z}_1 + \underline{Z}_2 \quad (11)$$

$$\underline{Z}_{BF} = \underline{Z}_4 + \underline{Z}_{LF} = \underline{Z}_4 + \underline{Z}_3 \quad (12)$$

In contrast to conventional distance protection impedance results, both the reactive and the resistive part of the impedance result can be used to allocate the results to a topographical fault location. The impedance results are unaffected by the fault impedance and equal for all types of unbalanced faults at fault location F and DER infeed situations. Additionally, positive-sequence and zero-sequence system actions before or during the whole fault period have no impact on the results likewise. An earth compensation factor like $\underline{Z}_E/\underline{Z}_L$ is not needed.
Equations (3) to (12) can be fed into a system of equations that is computed in the relay. In our exemplary case, this system of equations is appropriate for all faults in section A_N_{ref}. If a fault is detected within section B_N_{ref} a different system of equations is used. For any section of the ring, a system of equations must be prepositioned in the protection relay. According to the ring section derived from the faulty section decision logic, the proposed method then chooses the appropriate system of equations for the precise fault localization.

STARTING CONDITIONS

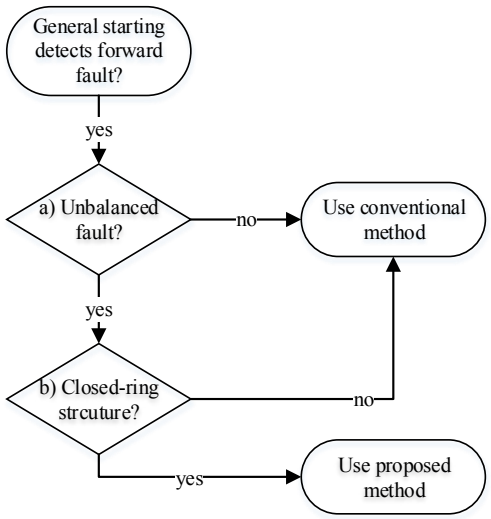

Fig. 4: Relay Starting Flow Chart with Proposed Method

The flow chart for the relay starting conditions of the current based method is shown in Fig. 4. The proposed method in this paper is adjusted to clear and locate unbalanced faults in closed-ring structures. If a system operation state complies with the general starting conditions of a busbar relay, the proposed methods checks if the fault is unbalanced. This is performed in Fig. 4 in decision block a) by comparing the absolute value of the sum of both relays' measured negative-sequence currents to a total negative-sequence current threshold $I_{sum,min(2)}$ according to condition (13). The threshold is defined by the DSO and must be set with respect to the actual grid environment where the proposed method is supposed to be installed in.

$$\left|\underline{I}_{A(2)} + \underline{I}_{B(2)}\right| > I_{sum,min(2)} \quad (13)$$

If condition (13) is true, the proposed method verifies if the ring is actually closed. This is performed in decision block b) in Fig. 4. The ring is considered to be closed, if each relay senses a significantly high absolute value of negative-sequence current according to condition (14).

$$\left|\underline{I}_{A(2)}\right| > I_{A,min(2)} \;\&\; \left|\underline{I}_{B(2)}\right| > I_{B,min(2)} \quad (14)$$

Condition (14) can only be true, when the ring is closed. If a tie switch is open, just one of the relays senses a significant negative-sequence current. Therefore, the proposed method inherently is disabled in case of an open ring. This means, no information on switching states along the ring is needed.
If any of the two conditions (13) or (14) is not true, the task of clearing and locating the fault is forwarded to conventional protection methods.

PROTECION GRADING STRATEGY

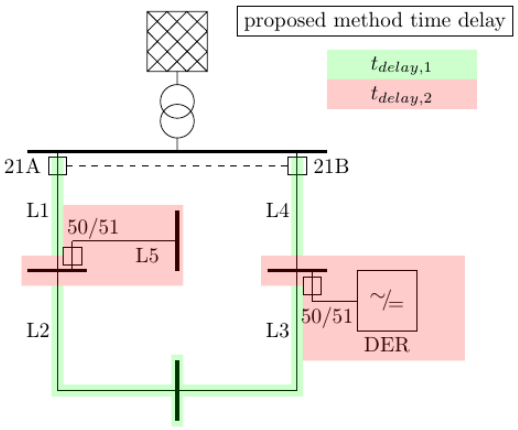

Fig. 5: Protection Grading with Proposed Method

As Fig. 1 shows, a protection system using conventional distance protection relays can lead to insufficient fault clearing times in closed-ring grids with distributed generation. Fig. 5 shows the improvement using the current based method proposed in this paper. The proposed method detects where *on the ring* the fault occurs, whereas conventional distance protection relays work on basis of detecting the mere impedance from the relay to the fault location. The proposed method figuratively "pulls" faults on lateral feeders to the node where the lateral feeder is connected to the ring. For Fig. 5, this means, all faults along the lateral feeder L5 lead to the same result as for a fault on the node where L5 is connected to the ring. Any impedance from that node to the actual fault location on the lateral feeders affects the magnitude and angle of the fault current only, but not way the fault current distributes in the ring in the negative-sequence system network

(cf. Fig. 2). Thus, the FCC remains unaffected. This means, in contrast to conventional distance protection methods, the proposed method can distinguish between faults on the ring and on lateral feeders. Consequently, the time delay can be set to $t_{delay,1}$ for faults on L2 and L3 and does not need be kept at the longer time delay $t_{delay,2}$ as it is the case for conventional distance protection (see Fig. 1). For faults on the lateral feeder L5 or inside the DER, the proposed method can provide backup protection for the respective time overcurrent protection relays. To avoid relay overfunction, a safety margin must be introduced around the nodes where L5 and the DER are connected to the ring. This means faults on the ring close to those nodes are cleared with $t_{delay,2}$.

When the proposed method is used, relays 21A and 21B share the same protection zones. Both circuit breakers may then be tripped via one signal deriving from the proposed methods results. Compared to the conventional distance protection grading strategy, the protection grading strategy for the proposed method leads to by far more green areas with shorter time delays. Thus, a shorter average fault clearing time can be achieved.

CONCLUSION

Since the proposed current based distance protection method works in a fundamentally different mode than conventional distance protection, it offers some operational unfamiliarities and characteristics. The following paragraphs state the most relevant features of the proposed method and important differences to the conventional distance protection method:

The proposed method is applicable in closed-ring structures exclusively and works for unbalanced faults only.

The FCC depends on the location where the fault current "enters" the ring and thus is independent from DER infeed in the positive-sequence system as well as from fault resistance and possible inaccuracies of zero-sequence quantities. It is equal for phase-to-ground, phase-to-phase and phase-to-phase-to-ground faults. This means, the determination of the faulty section and the calculation of the impedance between the relay and the fault location in the precise fault localization is very robust.

The proposed method detects faults on lateral feeders as if they would have occurred at the node where the lateral feeder is connected. This helps to distinguish faults on the ring from faults on lateral feeders. In contrast to conventional distance protection methods, the proposed method provides no impedance-wise indication, where on the lateral the fault location occurs. A combined usage of results from the current based method (*is the fault on the lateral feeder?*) and conventional distance protection methods (*where on the lateral feeder is it?*) might be suitable to improve fault locating on lateral feeders.

The proposed method can serve as a low-level fault locator in closed-ring structures. This is especially helpful, if the ring is equipped with non-directional short-circuit indicators. These short-circuit indicators are vulnerable to fail to operate properly in closed rings.

The proposed protection grading strategy can lower the average fault clearing time. Thus, the risk of loss of DER is lowered since faults are less likely to cause system states that violate FRT regulations.

The proposed method is not capable of clearing balanced faults and it cannot clear unbalanced faults in open ring structures, e.g. in post-fault or maintenance situations. Consequently, the proposed method cannot be a standalone solution but relays must be equipped with an additional protection algorithm in any case.

REFERENCES

[1] G. Ziegler, Numerical Distance Protection - Principles and Applications, 4th edition, Germany, 2011.

[2] Siemens AG, "SIPROTEC 5 - Relay Manual," Germany, 2017.

[3] M. Washer, J.-C. Maun, C. Dzienis, M. Kereit, Y. Yelgin and J. Blumschein, "Precise Impedance Based Fault Location Algorithm with Fault Resistance Separation," in *IEEE Power Tech*, Eindhoven, Netherlands, 2015.

[4] L. Eriksson, M. M. Saha and G. D. Rockefeller, "An Accurate Fault Locator With Compensation For Apparent Reactance in the Fault Resistance Resulting from Remote-End Infeed," *IEEE Transactions on Power Apparatus and Systems, Vol. PAS-104, No. 2,* pp. 424-436, February 1985.

[5] T. Takagi, Y. Yamakoshi, M. Yamaura, R. Konow and T. Matsushima, "Development of a New Type Fault Locator Using the One-Terminal Voltage and Current Data," *IEEE Transactions on Power Apparatus and Systems,* October 1982.

[6] J. Izykowski, E. Rosolowski and M. Mohan Saha, "Locating Faults in Parallel Transmission Lines Under Availability of Complete Measurements at One End," *IEE Proceedings - Generation, Transmission and Distribution,* pp. 268-273, 2 March 2004.

[7] M. Biller and J. Jaeger, "Relay Coordination of Highly Meshed Distribution Grids in the Presence of Volatile Infeed and Power Flow Control," in *APAP 2015 - The 6th International Conference on Advanced Power System Automation and Protection*, Nanjing, China, 2015.

[8] M. Biller and J. Jaeger, "Selective Protection Relaying in the Presence of Distributed Generation and Closed-Ring Structures," in *2018 International Conference on Power System Technology (POWERCON 2018*, Guangzhou, China, 2018.